



# Application of the comprehensive identification model in analyzing the source of water inrush

Qin Liu<sup>1,2</sup> · Yajun Sun<sup>1,2</sup> · Zhimin Xu<sup>1,2</sup> · Gang Xu<sup>3</sup>

Received: 14 November 2017 / Accepted: 16 April 2018 / Published online: 27 April 2018  
© Saudi Society for Geosciences 2018

## Abstract

Disasters caused by water inrush during production affect many coal mines in China. To rapidly and accurately prevent further water inrush, a comprehensive identification model combining hydrochemistry analysis, water source detection, and water channel exploration is proposed. The Shukalev classification method (SCM) is used to distinguish the concentration distribution of the main ion between the water inrush source and other aquifers, and hierarchical cluster analysis (HCA) is adopted to classify the water samples in the hydrochemistry analysis stage. Water channel exploration and water source detection are combined to test and verify the conclusion in the third stage. The comprehensive discrimination model is applied to the water inrush of the Buliangou coal mine. Hydrochemistry analysis shows that the percentages of the main ions ( $\text{Na}^+$ ,  $\text{Ca}^{2+}$ ,  $\text{Mg}^{2+}$ ,  $\text{HCO}_3^-$ , and  $\text{Cl}^-$ ) are greater than 30% (excluding  $\text{SO}_4^{2-}$ ), which is in agreement with the case of a sandstone aquifer. In the second stage, water source detection based on the transient electromagnetic method (TEM) and drilling technique indicates that not much water is present in the anomaly area around the water inrush location. The limited water recharge contradicts the phenomenon of water inrush. Water channel exploration is carried out, and an area with massive fissures that have water storage capacity is revealed. The conclusion is that the water conserved in the fissures flows out over a short time without the occurrence of stable recharge. The comprehensive discrimination model has complementary advantages and improves the water inrush prediction efficiency.

**Keywords** Coal mine · Hydrochemistry analysis · Hierarchical cluster analysis · Water source detection · Water channel exploration

## Introduction

Water inrush is of paramount concern to the mining industry (Wu et al. 2017; Hu et al. 2011; Yang et al. 2018). Water inrush has various causes and consequences, including catastrophic failure, substantial economic losses, and the loss of lives (Zhang 2005; Yang et al. 2017). Therefore, identifying sources of water inrush is of vital importance for progressing safety surveillance and maintenance. Hydrogeological and structural conditions, along with the corresponding water level, temperature, and hydrochemistry, are commonly used in the literature to comprehensively analyze and determine a water source. The hydrochemistry method originated from a simple water quality analysis and developed to isotope technology (Dou et al. 2011; Ma et al. 2015; Yao et al. 2016; Bo et al. 2015). Nonlinear analysis methods, including Grey system theory (Qiu et al. 2016; Xiao et al. 2013), fuzzy mathematics (Xiao et al. 2016; Peng et al. 2015), artificial neural networking (Wang et al. 2012), geographic information systems, and the support vector

✉ Yajun Sun  
syj@cumt.edu.cn

Qin Liu  
lq\_cumt@live.cn

Zhimin Xu  
xuzhimin@cumt.edu.cn

Gang Xu  
13934855750@163.com

<sup>1</sup> School of Resources and Geosciences, China University of Mining and Technology, Xuzhou 221116, China

<sup>2</sup> China National Water Disaster Control Research Institution, Xuzhou, China

<sup>3</sup> Inner Mongolia Mengtai Buliangou Coal Industry Co., Ltd., China Huadian Corporation, Ordos 017000, China

machine (Zhang et al. 2006), have also been studied and applied. The hydrochemistry method eventually evolved into multivariate statistical methods, which include cluster analysis (Sun 2014; Wang et al. 2011; Areerachakul and Sanguansintukul 2010) and discriminant analyses (Panagopoulos et al. 2016; Singaraja et al. 2014; Güler et al. 2002).

In the past few decades, hydrochemistry analysis, water source detection, and water channel exploration were proposed to analyze the source of water inrush individually. Each has its own shortcomings leading to misjudgments. Hierarchical cluster analysis (HCA) is typically performed to determine the source of water inrush in coal mines (Helstrup et al. 2007; Li et al. 2014). However, it is difficult to satisfy the requirements of safety in mining via hydrochemistry analysis due to water mixture and the severe threat of disaster. The aim of this paper is to analyze the reliability of the hydrochemistry method and then to propose a comprehensive identification model that is useful for preventing mine water hazards.

## Study area

### Buliangou coal mine

The Buliangou coal mine is located in the Dalu Township of the Inner Mongolia autonomous region. The study area is part

of the Yellow River basins, and the rivers in this area drain into the Yellow River seasonally. The land slopes gently towards the northeast. In addition, the ground level is generally between 1127 and 1346 m above sea level (Fig. 1).

The Buliangou coal mine has a temperate continental monsoonal climate and a mean annual temperature of 7.8 °C. The climate is arid; the average annual precipitation was 389.80 mm from 1961 to 2014. The average annual evaporation is 1964.8 mm. The study area is dominated by descending precipitation, and precipitation deficit may further worsen the shortage of water resources. The extreme precipitation events in this area have followed an increasing trend, which has been more noticeable over the past decade. In addition, a higher risk of drought can be expected in summer, and the amount of precipitation in winter and spring has been increasing. The coal mine is influenced by seasonal precipitation according to the relation curve of the mine water inflow (Huang et al. 2015).

### Geological conditions of panel F6204

The Buliangou coal mine is located in the northern Zhungeer coalfield. Panel F6204 is in the northwest region of the coal mine and is the first panel affected by the Ordovician limestone with confined water pressure. The strike length of the panel is 1330 m, while the inclination length is 240 m. The panel is geologically located in a

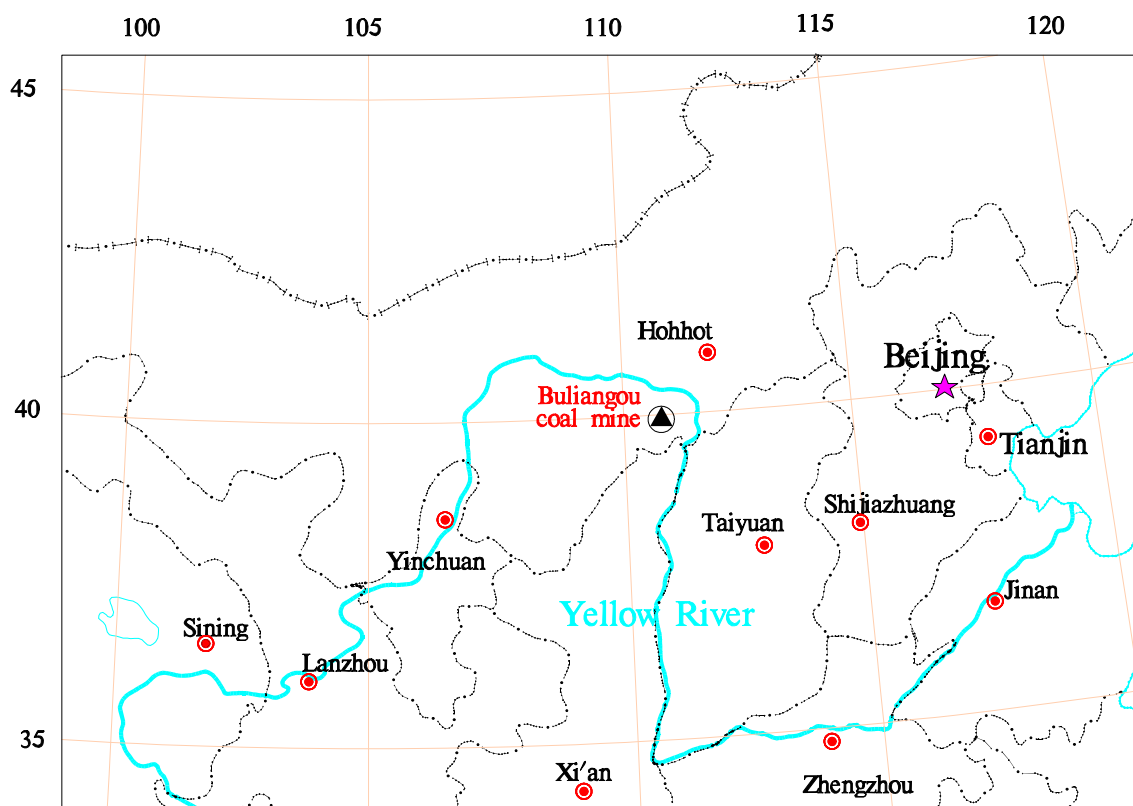


Fig. 1 Location of the Buliangou coal mine

monoclinical structure with five small faults and two large faults, namely, DF<sub>28</sub> and DF<sub>30</sub> (Fig. 2). The main water channels of panel F6204 might be these faults, the water flowing fractured zones, fissures, and an improperly sealed drill hole (Y0808). The water channels may cause a hydraulic interaction between the confined Ordovician limestone aquifers and the panels (Wu and Wang 2006; Xu and Gong 2011; Sun et al. 2008).

Previous research has shown that the aquifers that primarily affect the no. 6 coal seam include the sandstone aquifers of the Shanxi group (A<sub>1</sub>), those of the Taiyuan group (A<sub>2</sub>), and the karstic limestone aquifers of the Ordovician (A<sub>3</sub>), as shown in Fig. 3. The mean thickness of A<sub>1</sub> is 58.13 m, and the specific capacity is 0.007 L/s m. The thickness of A<sub>2</sub> varies from 34.95 to 89.45 m, the water level is 933.00 m, and the specific capacity is 0.008 L/s m. A<sub>3</sub> is an indirect water source of the no. 6 coal seam and located approximately 60 m below the floor. Its specific capacity is 1.581 L/s m. The floor elevation of this panel is generally between 822 and 904 m, and the water level of A<sub>3</sub> varies from 866.42 to 876.66 m. Panel F6203 is adjacent to panel F6204 on its north side. The accumulated water from panel F6203 could flow into panel F6204.

### Water inrush situation

There were two points of water inrush occurred at panel F6204, as shown in Fig. 2. The initial water discharge from the auxiliary transport gateway was 30 m<sup>3</sup>/h. The water inflow was constant at 5 m<sup>3</sup>/h after drainage. The water inflow through the main transport gateway was 23 m<sup>3</sup>/h. It was well known that there was a threat of water inrush in the process of mining the panel. The source of the water inrush, regardless whether it was the water of panel F6203 or the A<sub>3</sub> aquifer, was considered to pose a significant threat to mining safety (Li and Zhou 2006).

### Methodology

Determining water inrush sources without knowing the water pressure or flow field is difficult (Liu and Cao 2011). In this study, we developed a comprehensive discrimination model to assess water inrush according to the following three steps.

### Sampling and preliminary analysis

The hydrochemical characteristics of water samples from the Buliangou coal mine were analyzed and studied. Analysis of the water inrush samples was conducted at the Shanxi Provincial Coal Industry Bureau Testing Center via the following methods: SO<sub>4</sub><sup>2-</sup>, Cl<sup>-</sup>, (Na<sup>+</sup>+K<sup>+</sup>), Ca<sup>2+</sup>, and Mg<sup>2+</sup> were analyzed by ion chromatography (CIC-200); alkalinity (including HCO<sub>3</sub><sup>-</sup> and CO<sub>3</sub><sup>2-</sup>) was analyzed by acid-base titration (Papadopoulou-Vrynioti et al. 2014). Analyses of the ion chromatography were calibrated by the standard curve method, which was constructed based on the standard solution. All of the analyses had a relative standard deviation below 3%, and a hydrochemistry database was constructed (Bathrellos et al. 2008). Then, the Schukalev classification method (SCM) was used to analyze the concentration distribution of the main ion between the water inrush source and other aquifers (Jiang et al. 2006). Concentrations with anion and cation contents greater than 25% were categorized into 49 hydrochemical types, as shown in Table 1. Each type with a serial number denotes the hydrochemistry of the water sample itself.

### Hierarchy clustering analysis

HCA is adopted to classify the water samples. Each water sample that contained *m* test indexes is defined as a point in *m*-dimensional space (Anderberg 1973). The diverse distances between two categories result in different clustering results and the development of different clustering methods. The most common clustering methods include the nearest neighbor, the furthest

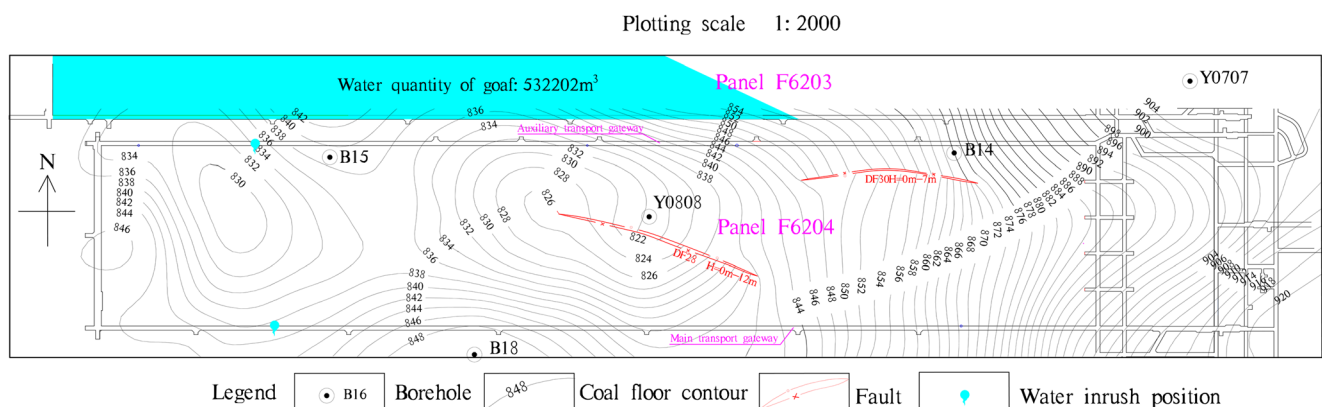


Fig. 2 Diagrammatic sketch of geological structure at panel F6204

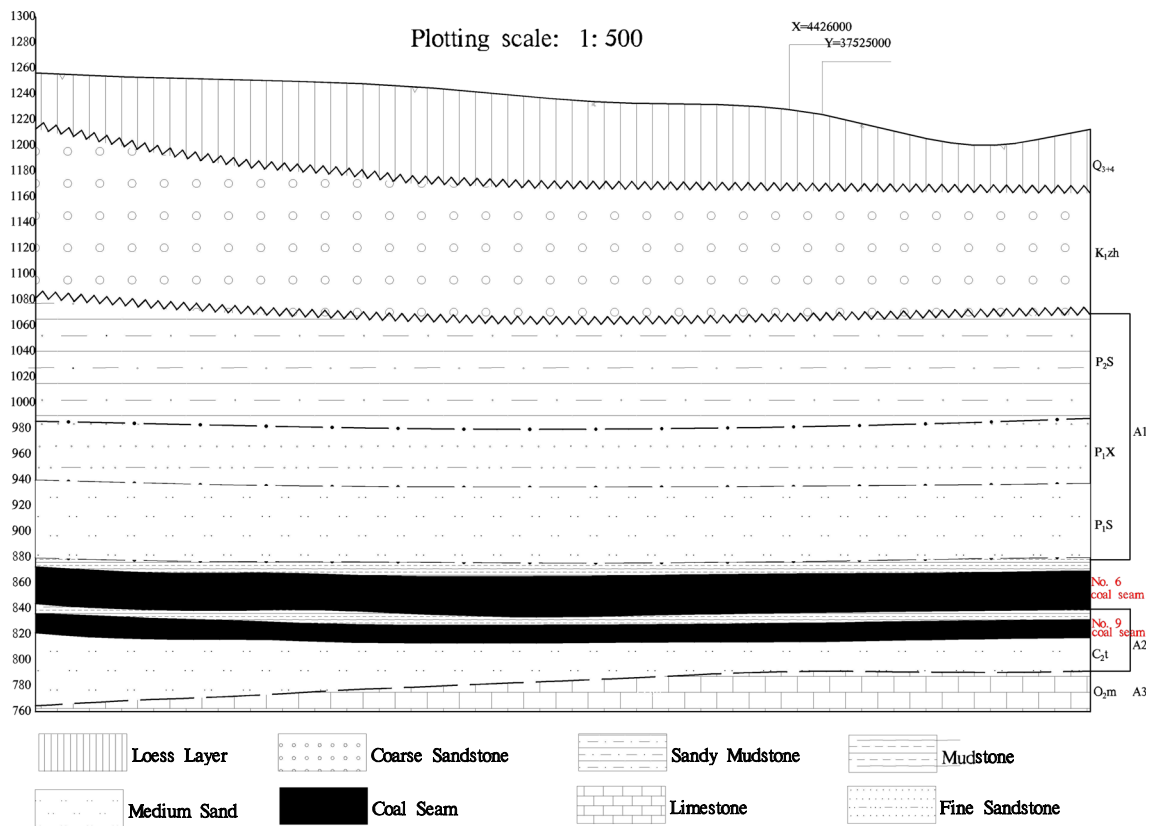


Fig. 3 Section plan of geological structure in panel F6204

neighbor, the between-group linkage, and Ward’s method. The higher the hydrochemical similarity between water inrush samples and standard water samples, the more accurate the results will be in determining the source of water inrush. Cluster identification by the nearest neighbor method, which was carried out in this paper, is shown to be quite reliable and robust with respect to the highest similarity, with the identified cluster being very consistent with those obtained via the SCM. The entire clustering process can be represented as a cluster graph (tree) image.

**Verification process**

Water inrush from the aquifer into the coal seam is affected by two factors: the water yield of the aquifer and the distribution of

the water channels (Wu et al. 2017). To test and verify the conclusion of the first step, water source detection based on the TEM and drilling technique is used to analyze the water yield condition of the anomaly area. In addition, the radio wave perspective method is adopted to detect the fissure and structures.

**Results and discussion**

**Preliminary analysis**

In this study, a total of 11 standard hydrochemical dates, which can represent the characteristic of each aquifer, were collected from 31 samples (Table 2). Sample 1 was taken from

Table 1 Hydrochemistry types of sampled water by SCM

Over 25% ion content	HCO <sub>3</sub> <sup>-</sup>	HCO <sub>3</sub> <sup>-</sup> + SO <sub>4</sub> <sup>2-</sup>	HCO <sub>3</sub> <sup>-</sup> + SO <sub>4</sub> <sup>2-</sup> + Cl <sup>-</sup>	HCO <sub>3</sub> <sup>-</sup> + Cl <sup>-</sup>	SO <sub>4</sub> <sup>2-</sup>	SO <sub>4</sub> <sup>2-</sup> + Cl <sup>-</sup>	Cl <sup>-</sup>
Ca <sup>2+</sup>	1	8	15	22	29	36	43
Ca <sup>2+</sup> + Mg <sup>2+</sup>	2	9	16	23	30	37	44
Mg <sup>2+</sup>	3	10	17	24	31	38	45
Na <sup>+</sup> + Ca <sup>2+</sup>	4	11	18	25	32	39	46
Na <sup>+</sup> + Ca <sup>2+</sup> + Mg <sup>2+</sup>	5	12	19	26	33	40	47
Na <sup>+</sup> + Mg <sup>2+</sup>	6	13	20	27	34	41	48
Na <sup>+</sup>	7	14	21	28	35	42	49



**Table 2** Hydrochemistry characteristic of water samples (unit, %)

Sample	Sample site	K <sup>+</sup>	Na <sup>+</sup>	Ca <sup>2+</sup>	Mg <sup>2+</sup>	Cl <sup>-</sup>	SO <sub>4</sub> <sup>2-</sup>	HCO <sub>3</sub> <sup>-</sup>	SCM (type)
1	River	0.46	20.78	53.73	25.02	7.19	3.74	87.44	Ca <sup>2+</sup> + Mg <sup>2+</sup> —HCO <sub>3</sub> <sup>-</sup> (T2)
2	F6106 fault	0.69	21.04	44.54	33.73	7.16	8.92	83.75	Ca <sup>2+</sup> + Mg <sup>2+</sup> —HCO <sub>3</sub> <sup>-</sup> (T2)
3	F6106 roof	0.51	22.41	46.69	40.39	7.91	13.49	78.04	Ca <sup>2+</sup> + Mg <sup>2+</sup> —HCO <sub>3</sub> <sup>-</sup> (T2)
4	F6204 roof	2.54	35.61	30.40	31.45	41.18	21.17	30.05	Na <sup>+</sup> + Ca <sup>2+</sup> +Mg <sup>2+</sup> —HCO <sub>3</sub> <sup>-</sup> + Cl <sup>-</sup> (T26)
5	F6204 main transport	1.46	29.35	39.61	29.58	35.17	17.91	39.50	Na <sup>+</sup> + Ca <sup>2+</sup> + Mg <sup>2+</sup> —HCO <sub>3</sub> <sup>-</sup> + Cl <sup>-</sup> (T26)
6	F6204 auxiliary transport floor	1.78	29.84	39.06	29.32	37.20	22.42	40.38	Na <sup>+</sup> + Ca <sup>2+</sup> + Mg <sup>2+</sup> —HCO <sub>3</sub> <sup>-</sup> + Cl <sup>-</sup> (T26)
7	F6204 auxiliary transport floor	1.50	28.98	39.85	29.67	36.90	21.48	41.62	Na <sup>+</sup> + Ca <sup>2+</sup> + Mg <sup>2+</sup> —HCO <sub>3</sub> <sup>-</sup> + Cl <sup>-</sup> (T26)
8	F6204 auxiliary transport inrush	1.48	37.69	36.44	24.27	37.58	23.34	39.01	Na <sup>+</sup> + Ca <sup>2+</sup> + Mg <sup>2+</sup> —HCO <sub>3</sub> <sup>-</sup> + Cl <sup>-</sup> (T26)
9	F6204 main transport inrush	0.88	35.57	34.25	39.24	34.81	25.31	39.81	Na <sup>+</sup> + Ca <sup>2+</sup> + Mg <sup>2+</sup> —HCO <sub>3</sub> <sup>-</sup> + SO <sub>4</sub> <sup>2-</sup> + Cl <sup>-</sup> (T19)
10	Ordovician limestone aquifer	0.68	32.07	33.97	33.29	16.69	26.32	54.00	Na <sup>+</sup> + Ca <sup>2+</sup> + Mg <sup>2+</sup> —HCO <sub>3</sub> <sup>-</sup> + SO <sub>4</sub> <sup>2-</sup> (T12)
11	F6208 roof	0.86	38.09	31.00	30.05	12.54	26.81	60.65	Na <sup>+</sup> + Ca <sup>2+</sup> + Mg <sup>2+</sup> —HCO <sub>3</sub> <sup>-</sup> + SO <sub>4</sub> <sup>2-</sup> (T12)
12	Drained hole D3 of F6203	1.10	52.23	25.89	20.70	24.45	22.39	50.73	Na <sup>+</sup> + Ca <sup>2+</sup> —HCO <sub>3</sub> <sup>-</sup> + Cl <sup>-</sup> (T25)
13	Drained hole D6 of F6203	1.04	53.44	26.18	19.34	29.07	19.23	51.21	Na <sup>+</sup> + Ca <sup>2+</sup> —HCO <sub>3</sub> <sup>-</sup> + Cl <sup>-</sup> (T25)

a nearby river, while samples 2 and 3 were collected from the roof of panel F6106. Samples 4, 5, 6, and 7 were taken from A<sub>2</sub>. Sample 10 was taken from A<sub>3</sub>. Sample 11 was taken from the roof of panel F6208. Samples 12 and 13 were taken from panel F6203. Samples 8 and 9 were collected at the locations of water inrush and sent to a laboratory for analysis of the main ions.

The water samples were classified via Schukalev classification method (SCM). We categorized the water samples into six groups: (1) Sample 1 was taken from the river, and the hydrochemical type was Ca<sup>2+</sup> + Mg<sup>2+</sup>—HCO<sub>3</sub><sup>-</sup>. (2) Samples 2 and 3 were taken from panel F6106, and the hydrochemical type was Ca<sup>2+</sup> + Mg<sup>2+</sup>—HCO<sub>3</sub>. (3) Samples 4, 5, 6, and 7 were taken from the transport gateway floor on both sides of panel F6204, with sampling locations in the A<sub>2</sub> of floor. The hydrochemical types were Na<sup>+</sup> + Ca<sup>2+</sup> + Mg<sup>2+</sup>—HCO<sub>3</sub><sup>-</sup> + Cl<sup>-</sup>. (4) Samples 8 and 9 fell into the same category, possibility originating from the A<sub>2</sub> aquifer. (5) Sample 10 was taken from A<sub>3</sub>, and the hydrochemical type was Na<sup>+</sup> + Ca<sup>2+</sup> + Mg<sup>2+</sup>—HCO<sub>3</sub><sup>-</sup> + SO<sub>4</sub><sup>2-</sup>. It can represent the characteristics of water from the A<sub>3</sub> aquifer. Sample 11 was taken from the A<sub>1</sub> aquifer, and the hydrochemical type was Na<sup>+</sup> + Ca<sup>2+</sup> + Mg<sup>2+</sup>—HCO<sub>3</sub><sup>-</sup> + SO<sub>4</sub><sup>2-</sup>. (6) Samples 12 and 13 were taken from panel F6203, and the hydrochemical type was Na<sup>+</sup>+Ca<sup>2+</sup>—HCO<sub>3</sub><sup>-</sup> + Cl<sup>-</sup>. The percentage of Na<sup>+</sup> and HCO<sub>3</sub><sup>-</sup> ions in samples 12 and 13 was high, being obtained from the goaf area, which has been contaminated by mining activity.

### Hierarchy clustering analysis

Groundwater contains different types and amounts of ions in different locations; hence, ionic components are often used to indicate the chemical characteristics of a water source (Helstrup et al. 2007). In this study, we applied seven common ions, Na<sup>+</sup>, K<sup>+</sup>, Ca<sup>2+</sup>, Mg<sup>2+</sup>, Cl<sup>-</sup>, SO<sub>4</sub><sup>2-</sup>, and HCO<sub>3</sub><sup>-</sup>, as the

indexes for clustering. The HCA model was established to determine the cluster distance ( $D_E$ ) of water inrush and the different groundwater hydrochemical characteristics. The calculation process is as follows.

- (1) The primary data of the seven indexes were processed by the standard deviation standardization method.
- (2) The Euclidean distance was used to measure the distance between 13 sets of water quality data. If the seven-dimensional space of any two samples in terms of the distance was calculated, this could be arranged in the distance similarity matrix as shown in Table 3.
- (3) The distance between classes was calculated by the nearest neighbor method, and the samples were classified. The samples were divided into three groups, as shown in Fig. 4.

Samples 1, 2, and 3 were placed in group 1. The hydrochemical type of group 1 is Ca<sup>2+</sup> + Mg<sup>2+</sup>—HCO<sub>3</sub><sup>-</sup>. The average contents of Ca<sup>2+</sup>, Mg<sup>2+</sup>, and HCO<sub>3</sub><sup>-</sup> were 48.32, 33.05, and 83.08%, respectively. Sample 1 was taken from the river, and the large volume of HCO<sub>3</sub><sup>-</sup> ions (the largest among all samples) shows that samples 2 and 3 had a close hydraulic relationship with the surface water.

Samples 10, 11, 12, and 13 were assigned to group 2. They could be further categorized, with samples 12 and 13 in group 2-1 and samples 10 and 11 in group 2-2. The percentage of Na<sup>+</sup> and HCO<sub>3</sub><sup>-</sup> ions is high in group 2-1, which is from the goaf area contaminated by mining activity. Thus, group 2-1 can represent the hydrochemical characteristics of the goaf water. Regarding group 2-2, sample 10 has a lower percentage of Cl<sup>-</sup> ions, and the percentages of the other ions are greater than 30%, with the SO<sub>4</sub><sup>2-</sup> ion content being greater than 50%. Sample 11 was taken from the A<sub>1</sub> aquifer, having

**Table 3** Similarity matrix of water sample

Similarity degree	1	2	3	4	5	6	7	8	9	10	11	12	13
1	1	0.999	0.989	0.647	0.865	0.841	0.865	0.469	0.435	0.935	0.801	0.624	0.612
2		1	0.987	0.642	0.866	0.844	0.866	0.477	0.454	0.945	0.823	0.638	0.620
3			1	0.690	0.881	0.857	0.881	0.521	0.479	0.929	0.813	0.693	0.689
4				1	0.568	0.537	0.568	0.347	0.493	0.530	0.514	0.396	0.415
5					1	0.998	1	0.733	0.647	0.931	0.778	0.725	0.732
6						1	0.998	0.725	0.638	0.930	0.765	0.713	0.718
7							1	0.733	0.647	0.931	0.778	0.725	0.732
8								1	0.924	0.551	0.737	0.847	0.869
9									1	0.514	0.775	0.777	0.777
10										1	0.848	0.700	0.672
11											1	0.883	0.841
12												1	0.993
13													1

hydrochemical characteristics similar to those of sample 10 from the A<sub>3</sub> aquifer but different from those of sample 4 of the A<sub>1</sub> aquifer. The abnormality of sample 11 indicates that it was greatly affected by the recharge of other aquifers; thus, group 2-2 can only represent the hydrochemical characteristics of the A<sub>3</sub> aquifer.

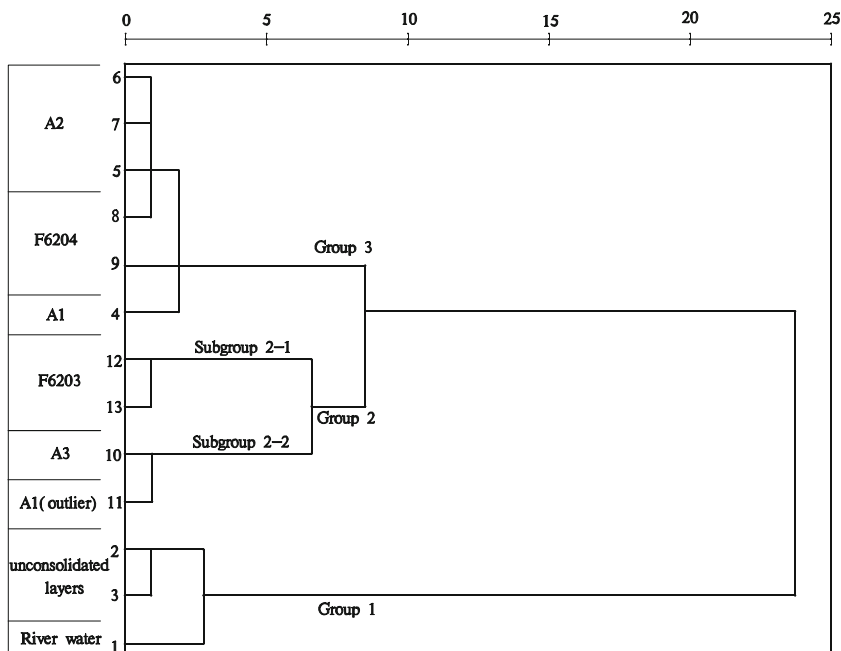
Samples 4–9 were classified as group 3. Aside from SO<sub>4</sub><sup>2-</sup>, the ion percentages are greater than 30%, which is the characteristic of water from the A<sub>2</sub> aquifer. It was obvious that samples of group 3 had a similar occurrence and hydrochemical characteristics to water originating from the A<sub>2</sub> aquifer.

The results of HCA can be explained by hydrochemical characteristic analysis. However, it is difficult to satisfy the requirements of safety in mining via hydrochemistry analysis due to water mixture and the severe threat of disaster.

**Verification process**

The result of SCA was consistent with that of HCA. The main ion characteristics of water samples determine the results of HCA. However, the occurrence and migration conditions of groundwater are the basis for the evolution of the ion

**Fig. 4** Dendrogram for cluster analysis of samples



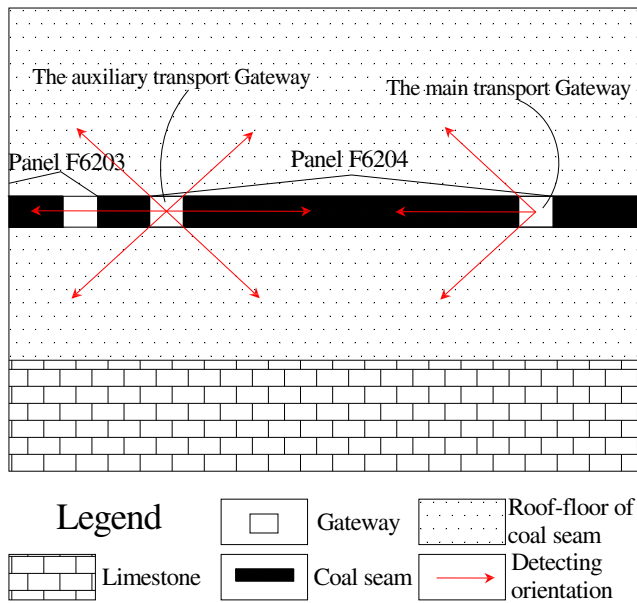


Fig. 5 Transient electromagnetic (TEM) detection orientation diagram

characteristics and decide the hydrochemical type fundamentally due to the water-rock interaction, which effect the conclusion of HCA based on the hydrochemical dates. To validate the accuracy of the above results, water source detection (the occurrence conditions) and water channel exploration (the runoff conditions) around the water inrush position are combined to clarify and verify the conclusion in the second stage.

### Water source detection

The TEM can provide a strong response for an underground conductive medium and is suitable for evaluating the degree of water in fault areas, detecting collapsed columns and classifying aquifers (Chang et al. 2016; Cheng et al. 2015). In this study, the TEM was used to detect the areas of anomalous water occurrence for panel F6204. The measuring points were arranged in the main transportation roadway and auxiliary transportation roadway of panel F6204, from the cut-hole to the stopping line, with a measuring point every 10 m, as shown in Fig. 5. The horizontal axis in Fig. 6 indicates the position along the gateway direction, while the vertical axis represents the distance along the direction of detection. The curve shows the apparent resistivity, with a unit of ohm meter. The TEM survey indicated two areas of low resistivity: from 130 to 270 m and from 600 to 780 m. The former shows low resistance in the transport gateway but not in the auxiliary gateway. As the elevation of the coal seam floor in this range was below the water level of A<sub>3</sub>, this range coincided with the location of the point of water inrush; this area was designated anomaly area I.

The latter showed a strong, low resistivity in both gateways and corresponded to the location of DF<sub>28</sub> and Y0808 in the panel; this area was designated anomaly area II. Figure 6a shows the result of anomaly area I, and Fig. 6b shows the

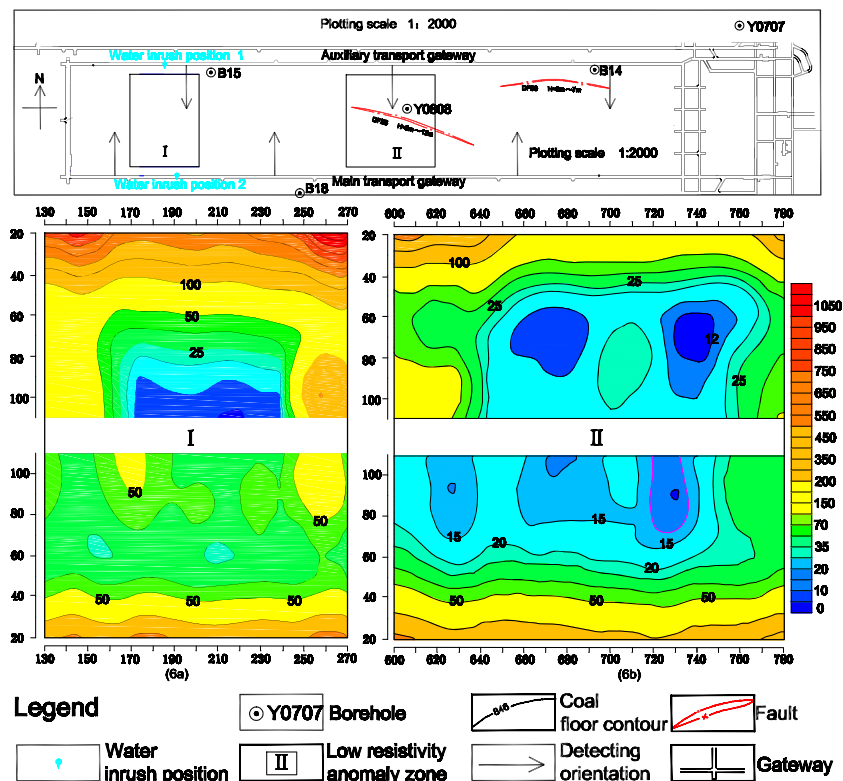


Fig. 6 Low resistivity anomalies obtained with transient electromagnetic (TEM) resistivity surveys

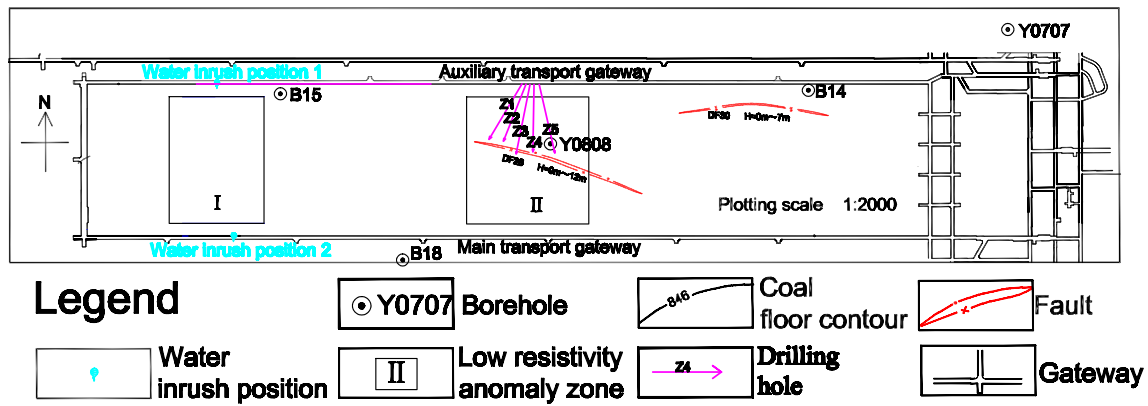


Fig. 7 Schematic diagram of drilling hole position in the anomalous area

result for anomaly area II. Anomaly area I had a half-open boundary, which indicated that the detected area had a large volume of water. Anomaly area II had a closed boundary, and the volume of water was greater than that of anomaly area I, which was supposed to be affected by the faults and the improperly sealed drill hole.

To further evaluate the degree of water in the anomaly area, five drill holes were created to detect the water in anomaly area II, as shown in Fig. 7 and Table 4. Drill hole Z<sub>5</sub> had a maximum water pressure of 0.16 MPa, whereas the water pressure could not be detected in the other drill holes. The drilling grouting pressure was expected to be 0.3 MPa if the water was derived from the A<sub>3</sub> aquifer. The results show that the supply of water in anomaly area II was limited.

### Water channel exploration

The radio wave perspective method is a geophysical technique that uses electromagnetic waves to characterize coal seam waveguides, through which the geological structure of coal seams can be examined (Xiao et al. 2016). An area K<sub>1</sub>, with mainly vertical fissures, was discovered, as shown in Fig. 8.

The huge fissure network provides a good space for groundwater movement and storage. Two positions of water inrush were found in the K<sub>1</sub> area on both sides, which overlap

with anomaly area I. This indicated that the source of inrush at panel F6204 was the A<sub>2</sub> aquifer.

### Further discussion

SCA has been used to find the significant parameters that affect the hydrochemical characteristics of groundwater in each aquifer. In addition, HCA led to classification of the water samples into three groups. However, the results might not reflect the real hydrochemical characteristics due to mixture of the water samples and the use of different testing equipment. In this study, the hydrochemical characteristics of sample 11 were similar to those of sample 10, with the two samples originating from different aquifers. Even if the results of the hydrochemical methods were consistent, they might only result in a reference conclusion because of the severe threat of disaster. To avoid incorrect conclusions and reduce the chance of sample misplacement, other detection means are introduced.

The factors resulting in water hazards mainly include the yield of water sources and the scale of water channels. In the third stage, water source detection based on the TEM and drilling technique indicates that the occurrence of water in the anomaly area around the water inrush location is minimal. The limited water recharge contradicts the phenomenon of water inrush. Water channel exploration was carried out, with an anomaly area with massive fissures that have the capacity

Table 4 Technical parameters of drilling and data for water discharge

Borehole name	Azimuth (°)	Dip angle (°)	Depth (m)	Prediction of orifice pressure (MPa)	Flux (m <sup>3</sup> /h)	Measured orifice pressure (MPa)
Z1	209	- 8.67	135	0.30	0.027	No pressure
Z2	187	- 15.09	120	0.30	0.028	No pressure
Z3	164	- 7.17	140	0.30	0.360	No pressure
Z4	159	- 14.26	125	0.30	0.400	No pressure
Z5	155	- 24.59	130	0.30	1.500	0.160

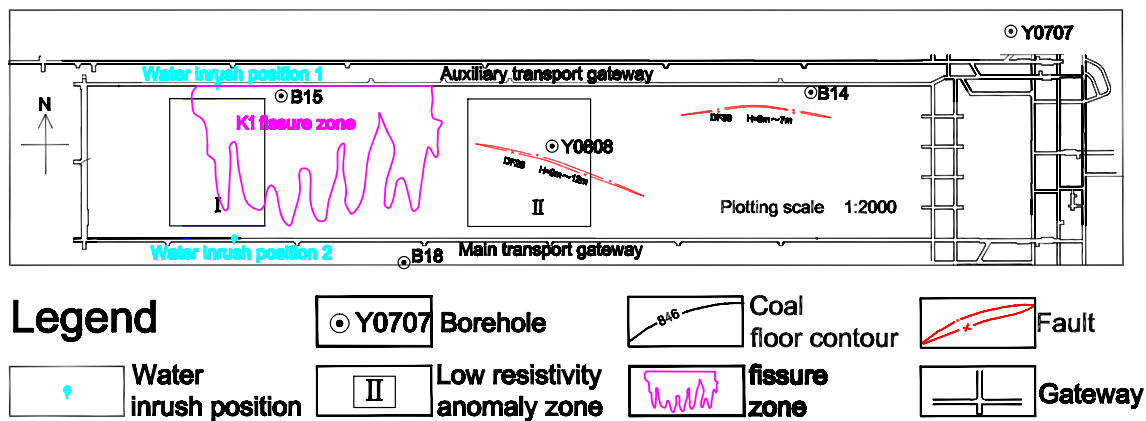


Fig. 8 Fissure development identification by the radio wave tunnel perspective method

for water storage being revealed. The combined water source detection and water channel exploration indicates that the water of the  $A_2$  aquifer conserved in these fissures flows out over short time but does not result in stable recharge. When the cation exchange reaction between the  $Ca^{2+}$ ,  $Mg^{2+}$ , and  $Na^+$  occurring on the surface of particle, the average concentration of  $Ca^{2+}$  and  $Mg^{2+}$  reduced by 24 and 7%, respectively, while that of  $Na^+$  increased by 53%. Due to the abundant  $Cl^-$  in the sandstone, the  $Cl^-$  in the groundwater raised by four times after filtration. Then, the water quality type changed from “ $Ca^{2+} + Mg^{2+} - HCO_3^-$ ” to “ $Na^+ + Ca^{2+} + Mg^{2+} - HCO_3^- + Cl^-$ ” which can represent the characteristics of water from  $A_2$ . Water inrush in the  $A_2$  aquifer flowed through the fracture and did not involve other aquifers; thus, the main ion characteristics were kept stable. HCA is suitable for analyzing the sources of water inrush in the Buliangou coal mine. The comprehensive discrimination model has complementary advantages and improves the water inrush prediction efficiency.

## Conclusions

Based on hydrochemical analyses of the major ion concentrations of groundwater samples from the Buliangou coal mine, a comprehensive identification model combining hydrochemistry analysis, water source detection, and water channel exploration is proposed and applied to identify the water inrush sources of the Buliangou coal mine. The following conclusions are obtained:

- (1) The groundwater samples from  $A_1$ ,  $A_2$ , and  $A_3$  are different from each other. The hydrochemical types of water inrush samples 8 and 9 were all  $Na^+ + Ca^{2+} + Mg^{2+} - HCO_3^- + Cl^-$ , being the same as that of the  $A_2$  aquifer. The possibility of water recharge from panel F6203 and the  $A_3$  aquifer was eliminated.
- (2) The ion characteristics of water samples determine the results of HCA. The occurrence (water sources) and

runoff conditions (water channel) are the basis for the evolution of the ion characteristics of groundwater.

- (3) The results show that the water of the  $A_2$  aquifer conserved in the fissures flows out over a short time but without stable recharge. The hydrochemistry analysis is reliable and accurate for water inrush prediction and can be used preferentially in emergency conditions for this coal mine. When the comprehensive identification model has been applied successfully, HCA would be enough for identification of water source. The use of the comprehensive identification model can be helpful for methods complementary and improving the prediction efficiency.

**Funding information** The authors acknowledge the financial support from the National Basic Research Program of China (973) Funded Project (Grant No. 2013CB227900) and the National Key R&D Program of China (Grant No. 2017YFC0804101).

## References

- Anderberg MR (1973) Cluster analysis for applications. Probability & mathematical statistics New York Academic Press
- Areerachakul S and Sanguansintukul S (2010) Clustering analysis of water quality for canals in Bangkok, Thailand. Computational Science and ITS Applications—ICCSA 2010, International Conference, Fukuoka, Japan, March 23–26, 2010, Proceedings. DBLP, 2010: 215–227
- Bathrellos GD, Skilodimou HD, Kelepertsis A, Alexakis D, Chrisanthaki I, Archonti D (2008) Environmental research of groundwater in the urban and suburban areas of Attica region, Greece. Environ Geol 56(1):11–18
- Bo Y, Liu C, Zhao Y, Wang L (2015) Chemical and isotopic characteristics and origin of spring waters in the Lanping–Simao basin, Yunnan, southwestern China. Chemie der Erde—Geochemistry—Interdisciplinary Journal for Chemical Problems of the Geosciences and Genealogy 75(3):287–300
- Chang JH, Yu JC, Liu ZX (2016) Three-dimensional numerical modeling of full-space transient electromagnetic responses of water in goaf. Appl Geophys 13(3):539–552



- Cheng J, Li F, Peng S (2015) Joint inversion of TEM and DC in roadway advanced detection based on particle swarm optimization. *J Appl Geophys* 123:30–35
- Dou H, Ma Z, Cao H, Feng L, Hu W, Li T (2011) Application of isotopic and hydro-geochemical methods in identifying sources of mine intruding water. *Int J Min Sci Technol* 21(3):319–323
- Güler C, Thyne GD, McCray JE, Turner KA (2002) Evaluation of graphical and multivariate statistical methods for classification of water chemistry data. *Hydrogeol J* 10(4):455–474
- Helstrup T, Jorgensenet NO, Banoeng-Yakubal B (2007) Investigation of hydrochemical characteristics of groundwater from the Cretaceous-Eocene limestone aquifer in southern Ghana and southern Togo using hierarchical cluster analysis. *Hydrogeol J* 15(5):977–989
- HU W, Dong S, Yan L (2011) Water hazard control technology for safe extraction of coal resources influenced by faulted zone. *Procedia Earth Planet Sci* 3:1–10
- Huang J, Sun S, Xue Y, Zhang J (2015) Changing characteristics of precipitation during 1960–2012 in Inner Mongolia, northern China. *Meteorol Atmos Phys* 127(3):257–271
- Jiang XY, Yu ZG, Ning JS, Chen HT, Mi TZ (2006) Genesis of underground brine along south coast of Laizhou Bay: hydrochemical characteristics. *Chin J Oceanol Limnol* 24(4):435–442
- LI G, Wang X, Meng Z, Zhao H (2014) Seawater intrush assessment based on hydrochemical analysis enhanced by hierarchy clustering in an undersea goldmine pit, China. *Environ Earth Sci* 71(12):4977–4987
- Li G, Zhou W (2006) Impact of karst water on coal mining in North China. *Environ Geol* 49(3):449–457
- Liu H, Cao Y (2011) Technologies of preventing coal mine water hazards for sustainable development in North China. *Geotech Geol Eng* 29(1):1–5
- Ma F, Zhao H, Guo J (2015) Investigating the characteristics of mine water in a subsea mine using groundwater geochemistry and stable isotopes. *Environ Earth Sci* 74(9):1–13
- Panagopoulos G, Angelopoulou D, Tzirtzilakis E (2016) The contribution of cluster and discriminant analysis to the classification of complex aquifer systems. *Environ Monit Assess* 181(10):591
- Peng K, Li X, Wang Z (2015) Hydrochemical characteristics of groundwater movement and evolution in the Xinli deposit of the Sanshandao gold mine using FCM and PCA methods. *Environ Earth Sci* 73(12):1–16
- Papadopoulou-Vrynioti K, Alexakis D, Bathrellos GD, Skilodimou HD, Vryniotis D, Vasiliades E (2014) Environmental research and evaluation of agricultural soil of the Arta plain, western Hellas. *J Geochem Explor* 136:84–92
- Qiu M, Shi L, Teng C, Zhou Y (2016) Assessment of water intrush risk using the fuzzy Delphi analytic hierarchy process and Grey relational analysis in the Liangzhuang Coal Mine, China. *Mine Water Environ* 1–12
- Singaraja C, Chidambaram S, Prasanna M, Thivya C (2014) Statistical analysis of the hydrogeochemical evolution of groundwater in hard rock coastal aquifers of Thoothukudi district in Tamil Nadu, India. *Environ Earth Sci* 71(1):451–464
- Sun L (2014) Statistical analysis of hydrochemistry of groundwater and its implications for water source identification: a case study. *Arab J Geosci* 7(9):3417–3425
- Sun YJ, Xu ZM, Dong QH et al (2008) Forecasting water disaster for a coal mine under the Xiaolangdi reservoir. *China Univ Mining Technol* 18(4):516–520
- Wang J, Li X, Cui T, Yang J (2011) Application of distance discriminant analysis method to headstream recognition of water-bursting source. *Procedia Eng* 24(6):374–381
- Wang J, Zhong H, Feng L (2012) A model of coal mine water disaster emergency logistics risk assessment based on AHP and BP neural network. *Future Communication, Computing, Control and Management*:535–542
- Wu Q, Wang M (2006) Characterization of water bursting and discharge into underground mines with multilayered groundwater flow systems in the North China coal basin. *Hydrogeol J* 14(6):882–893
- Wu Q, Guo X, Shen J et al (2017) Risk assessment of water intrush from aquifers underlying the Gushuyuan coal mine, China. *Mine Water & the Environment* 36(1):1–8
- Xiao L, Tang SH, Zhao CL, Yuan TX, Yang W (2013) Grey-risk estimation of the water intrush from no. 9 coal floor in Guoerzhuang mine. *Appl Mech Mater* 295-298:3019–3022
- Xiao Y, Wu R, Zhang P et al (2016) Application of radio wave penetration field strength increment method in detection by coal face roadway. *Min Saf Environ Prot* 36-40(In Chinese)
- Xu C, Gong P (2011) Water disaster types and water control measures of Hanxing coal mine area. *Procedia Earth Planet Sci* 3(3):343–348
- Yang B, Wanghua S, Lihong D (2017) Risk assessment of water intrush in an underground coal mine based on GIS and fuzzy set theory. *Mine Water Environ* 36(4):617–627
- Yang B, Junhong Y, Lihong D (2018) Development of a system to assess vulnerability of flooding from water in karst aquifers induced by mining. *Environ Earth Sci* 77(3):91–104
- Yao M, Liu P, Shang M, Tao Y, Lei C, Cao L (2016) Determining sources of mine water based on hydraulic characteristics analysis of a fault system. *Environ Earth Sci* 75(10):858
- Zhang J (2005) Investigations of water intrushes from aquifers under coal seams. *Int J Rock Mech Min Sci* 42(3):350–360
- Zhang ZG, Zhang HR, Du PJ (2006) Application of SVM in analyzing the headstream of gushing water in coal mine. *China Univ of Mining & Tech* 16(4):433–438